J. Fluid Mech. (1980), *vol.* 98, *part* 3, *pp.* 587–607
Printed in Great Britain

A model of confined thermal convection driven by non-uniform heating from below

By PETER D. KILLWORTH
Department of Applied Mathematics and Theoretical Physics,
University of Cambridge, England

AND PETER C. MANINS
Division of Atmospheric Physics, C.S.I.R.O., P.O. Box 77,
Mordialloc, Victoria 3195, Australia

(Received 27 March 1979 and in revised form 13 September 1979)

A model is presented of the two-dimensional boundary-layer and interior flow in a rectangular box resulting from the application of a quadratic temperature variation on its lower surface. The other walls are insulating. It is shown that a similarity form exists for the narrow, thermocline-like layer near the lower surface, and that this can satisfy all known consistency conditions with the interior, together with either laminar or turbulent side-wall regions. The interior temperature and Nusselt number are shown to be insensitive to Prandtl number, and to be primarily functions of the horizontal Rayleigh number Ra_L.

Specifically, the interior temperature, relative to the coldest applied value, is 60 % of the total applied temperature range. The Nusselt number is predicted to vary as $0{\cdot}26Ra_L^{\frac{1}{4}}$ for a box with unit aspect ratio. The dynamics of the side-wall region, and the details of the imposed temperature variation appear to be unimportant in determining the overall buoyancy exchange. The solutions are compared with numerical and observational results, and generally good agreement is found.

1. Introduction

A feature of most geophysical convection systems is that the heating and cooling responsible for motion is impressed non-uniformly at the upper or lower boundaries. The result is a strongly asymmetric circulation. Thus, for example, the earth's oceans are cooled most strongly at high latitudes, and it is there that most of the bottom water is formed, with weak upwelling elsewhere. The atmosphere's Hadley-cell circulation is driven by heat transfer from the warmer surface at equatorial latitudes compared with more temperate latitudes.

Following up the ideas put forward by Stommel (1950, 1962), Rossby (1965) studied by laboratory experimentation the archetypal problem of interest here. A long rectangular box, insulated on all faces except the bottom, was heated so as to maintain a steady linear temperature increase with distance along that face. Rossby observed the circulation set up and measured temperature profiles to determine the efficiency of heat transfer. He observed that the heat exchange of the fluid with the lower boundary occurred in a thin boundary layer, the flow in which was directed toward the hotter end of the cell. There it rose against the wall, forming a line plume, flowed

0022-1120/80/4464-1140 $02.00

along the upper surface in a thicker layer and was then advected through a remarkably well-characterized broad interior region toward the lower boundary. 'The interior is advectively warmed, hence its temperature is an average of the warm fluid supplying it. The heat is withdrawn from it by forcing the warm fluid (by continuity) down against the bottom where it is cooled by conduction. Hence the asymmetry is just a measure of the efficiency by which heat is transported by convection and conduction' (Rossby 1965). Two significant results obtained were that the interior was relatively quiescent and weakly stably stratified in temperature, and characterized by a temperature excess which was about 70% of the maximum temperature difference imposed at the bottom.

Subsequently, Somerville (1967), Beardsley & Festa (1972) and McKenzie, Roberts & Weiss (1973) numerically treated problems similar to that studied by Rossby. Although detailed comparison with the laboratory results is not possible, because each numerical analyst used different boundary conditions and had difficulty achieving sufficiently large Rayleigh numbers, all remark on the qualitative similarities with Rossby's work and the lack of sensitivity the results display with respect to variation of Prandtl number.

Scale analyses which presumably hold to very large Rayleigh numbers have been detailed by Rossby (1965), Goody & Robinson (1966) and Stone (1968), although the latter two studies are concerned with the problem of no friction at the diabatic surface. Further, Duncan (1966) has solved a similar problem in axisymmetric co-ordinates with strong rotation, by the method of matched asymptotic expansions. Stern (1975) discusses Rossby's problem, but mainly for strongly rotating fluids.

We present here a new solution to Rossby's archetypal problem, drawing on a recent study of convection in a box driven by a discrete buoyant plume at one end (Manins 1979) to justify the approach taken. Thus we accept that the fluid in the lower boundary layer, first cooled and then heated as it flows toward the hotter end, is able to turn upwards there and correctly supply the narrow wall plume. (Wesseling (1969) has studied the turning region in detail for the case of Bénard convection.) At sufficiently high Rayleigh numbers the plume is turbulent. This plume, together with the region where the plume flows out along the upper boundary in a thick layer, and the interior or core region, have been studied by Manins (1979) while the passive boundary layer on the colder wall has been studied by Walin (1971). The existence of these boundary layers on cold and hot walls gives consistency conditions on the remainder of the flow, which the solution derived here satisfies.

In this paper we concentrate on the lower boundary layer and the interior of the box. The forms of the characterizing stream function and buoyancy field for the interior are specified up to unknown coefficients and, in the course of solving for the boundary-layer functions, these will be evaluated. Now, the maximum and minimum temperatures are found at opposite ends of the bottom of the box; this factor is probably more important in determining the form of the solution than the shape of the impressed temperature field. Thus we feel free to depart from a linear temperature distribution, and look for one which admits similarity solutions to the boundary-layer stream function and buoyancy field.

Two problems will be solved. In both cases, the imposed temperature distribution for similarity solutions to be possible is one which increases as the square of distance from the colder end. (i) For low (but not too low) Rayleigh number, the rising plume

is laminar with negligible horizontal motion in the interior. (ii) At higher Rayleigh number, the plume becomes turbulent, with significant entrainment from the interior. A possible limitation on the maximum relevant Rayleigh number for this latter problem is the assumption that the *lower* boundary layer remains essentially laminar and does not spontaneously break up before the hotter end of the cell is reached. We do not ask that the lower layer *be* laminar, merely that it is reasonable to treat it in terms of a constant diffusivity. Spontaneous break-up of the layer would be inhibited by interior subsidence into the layer, and by the horizontal pressure gradient which helps to sweep (laminar or turbulent) fluid in the boundary layer towards the plume, where it can rise. With this proviso, there is no upper bound to the Rayleigh number in this model.

2. The mathematical model

Consider the steady two-dimensional flow in a box of length L and height H (figure 1). Define axes x horizontal, z vertical with origin at the cooler, left-hand end of the lower surface. The fluid density at the origin is ρ_1 and the buoyancy at a point where the density is ρ is defined by

$$\Delta' = -g\frac{\rho-\rho_1}{\rho_1}, \tag{2.1}$$

where g is the acceleration due to gravity. Primes will denote dimensional dependent variables. While all other surfaces are insulated, the boundary $z = 0$ is considered to be no-slip and maintained at a buoyancy given by

$$\Delta'_B = \Delta_m(x/L)^p, \tag{2.2}$$

where Δ_m is the buoyancy at the hotter, right-hand end of the bottom, and p will be specified by the demand for similarity solutions to be obtainable.

The equations of motion are then

$$\nu\nabla^4\psi' = \Delta'_x - J(\psi', \nabla^2\psi'), \tag{2.3a}$$

$$\kappa\nabla^2\Delta' + J(\psi', \Delta') = 0. \tag{2.3b}$$

Equation (2.3a) is the vorticity equation, (2.3b) the buoyancy equation, and ν and κ are respectively the kinematic viscosity and diffusivity of temperature in the fluid. ∇^2 denotes the two-dimensional Laplacian. The stream function ψ' is defined by

$$u' = \partial\psi'/\partial z, \quad w' = -\partial\psi'/\partial x. \tag{2.4}$$

These equations may be scaled as follows (Rossby 1965). Let $\delta \ll H$ be the bottom boundary-layer thickness (for both ψ and Δ), and set

$$\left.\begin{aligned} (x,z) &= (L\xi, H\zeta \equiv \delta\eta), \\ \Delta' &= \Delta_m\Delta, \quad \psi' = \kappa Ra_L^{\frac{1}{4}}\psi, \\ \delta &= L\,Ra_L^{-\frac{1}{4}}, \quad Ra_L = \Delta_m L^3(\nu\kappa)^{-1}. \end{aligned}\right\} \tag{2.5}$$

Here Ra_L is the boundary-layer Rayleigh number, assumed large, and we will introduce the Prandtl number $\sigma = \nu\kappa^{-1}$, assumed of order unity.

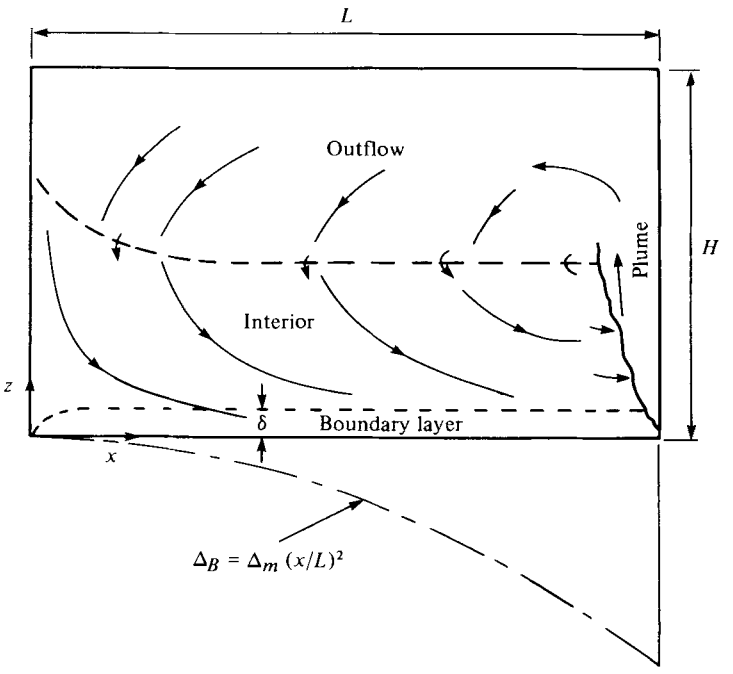

FIGURE 1. Sketch of the model, with a quadratic buoyancy distribution maintained at the surface $z = 0$. The case of a turbulent side-wall plume is shown.

The scaled form of (2.3) is

$$-\frac{1}{\sigma}\frac{\partial(\psi, Ra_L^{-\frac{2}{5}}\psi_{\xi\xi}+\psi_{\eta\eta})}{\partial(\xi,\eta)} - Ra_L^{-\frac{4}{5}}\frac{\partial^4\psi}{\partial\xi^4} - 2Ra_L^{-\frac{2}{5}}\frac{\partial^4\psi}{\partial\xi^2\partial\eta^2} = \frac{\partial^4\psi}{\partial\eta^4} - \frac{\partial\Delta}{\partial\xi}, \tag{2.6a}$$

$$\frac{\partial(\psi,\Delta)}{\partial(\xi,\eta)} + \frac{\partial^2\Delta}{\partial\eta^2} = -Ra_L^{-\frac{2}{5}}\frac{\partial^2\Delta}{\partial\xi^2}, \tag{2.6b}$$

whereas, in the interior, equations (2.3) reduce, for large Ra_L, to

$$\frac{\partial\Delta}{\partial\xi} = O(Ra_L^{-\frac{4}{5}}, Ra_L^{-\frac{3}{5}}\sigma^{-1}) \quad \text{or} \quad \frac{\partial\Delta}{\partial\xi} \sim 0, \tag{2.7a}$$

$$\frac{\partial(\Delta,\psi)}{\partial(\xi,\zeta)} = O(Ra_L^{-\frac{1}{5}}LH^{-1}) \quad \text{or} \quad \frac{\partial(\Delta,\psi)}{\partial(\xi,\zeta)} \sim 0. \tag{2.7b}$$

Two interior solutions are possible. However, the solution with

$$\frac{\partial\Delta}{\partial\xi} = w = -\frac{\partial\psi}{\partial\xi} = 0; \quad \frac{\partial\Delta}{\partial\zeta} \neq 0; \quad u = \frac{\partial\psi}{\partial\zeta} \neq 0$$

must be rejected on two grounds. First, Hignett (1979) found only a very weak vertical thermal gradient in his experiments (Rossby's 1965 experiments were far less well insulated). Secondly, the boundary condition in appendix A, and this interior solution, together imply zero net mass flux in the bottom boundary layer. This in turn forces a region of return flow toward the cold end in this layer, which is physically unreasonable and not observed in any experiments. We therefore choose the other interior solution, in which $\partial\Delta/\partial\zeta$ vanishes also, so that the interior is isothermal.

Away from the immediate vicinity of the side-walls, $Ra_L^{-\frac{2}{5}}\partial^2/\partial\xi^2$ is negligible compared with $\partial^2/\partial\eta^2$, and the bottom boundary-layer equations become

$$-\frac{1}{\sigma}\frac{\partial(\psi,\psi_{\eta\eta})}{\partial(\xi,\eta)} = \frac{\partial^4\psi}{\partial\eta^4} - \frac{\partial\Delta}{\partial\xi}, \tag{2.8a}$$

$$\frac{\partial(\psi,\Delta)}{\partial(\xi,\eta)} + \frac{\partial^2\Delta}{\partial\eta^2} = 0, \tag{2.8b}$$

with
$$\Delta = \xi^p, \quad \psi = \partial\psi/\partial\eta = 0, \quad \eta = 0. \tag{2.9}$$

Equations (2.8*a*, *b*) are second order in ξ, and require in general two boundary conditions to be satisfied. These must be obtained from consideration of the boundary layers on $\xi = 0$ and 1, the cold and hot walls respectively. Appendix A discusses these layers, and shows that

$$\psi = 0, \quad \xi = 0. \tag{2.10}$$

For laminar side-wall layers, it does not seem possible to derive a consistency condition on the hot wall, since the fluid turns in an essentially viscous, inertial corner region, in which diffusion is of secondary importance; uniqueness and existence of such problems remains an open subject (Batchelor 1967, pp. 285–288). The case of a turbulent side-wall layer is dealt with below.

Equations (2.8*a*, *b*) are now specified if ψ, Δ are known for $\eta \to \infty$, i.e. in the interior of the box (figure 1). Now for $\sigma > 1$, $L/H > 1$, and Ra_L sufficiently large for the plume to be turbulent, Manins (1979) has shown that the interior stream function ψ_I to a good approximation is given by

$$\psi_I \propto \xi(\zeta - \zeta_0), \tag{2.11a}$$

where ζ_0 is the virtual origin of the turbulent plume emanating from an equivalent discrete source. The flow in the interior is a stagnation flow. The interior buoyancy field is weakly stably stratified with horizontal isotherms and is well characterized for the present purpose by a constant Δ_I. At lower Ra_L the plume is laminar and the interior stream function below a stagnation-flow-like outflow region is then

$$\psi_I \propto \xi. \tag{2.11b}$$

That is, the flow in the interior is predominantly pure subsidence. The interior buoyancy is again characterized by a constant Δ_I. Thus we impose the boundary conditions that

$$\left.\begin{aligned} &\text{as} \quad \eta \to \infty, \quad \Delta \sim \Delta_I + f_n(\xi,\zeta); \\ &\text{and for a laminar plume, case (i),} \qquad \psi \sim \psi_I \propto \xi; \\ &\text{or for a turbulent plume, case (ii),} \qquad \psi \sim \psi_I \propto \xi(\zeta - \zeta_0). \end{aligned}\right\} \tag{2.12}$$

Similarity solutions to equations (2.8) subject to (2.9)–(2.12) are sought which retain all the essential nonlinearities of equations (2.8) while yet simplifying the system to a set of ordinary differential equations. It is found that such solutions are possible if

$$\left.\begin{aligned} &\psi = \xi^{(3+p)/5} f(\chi), \quad \Delta = \xi^p g(\chi) + k(\chi), \\ &\chi = \eta/\xi^{(2-p)/5}. \end{aligned}\right\} \tag{2.13}$$

Comparison of (2.13) and (2.12) as $\eta \to \infty$ gives $p = 2$ and $g(\chi \to \infty) = 0$ so that the boundary-layer thickness, from (2.13*c*), is independent of ξ. The flow towards a

'stagnation point' at a rigid boundary (a special case of the Falkner–Skan problem; Goldstein 1965, chap. IV) gives rise to a boundary layer with similar behaviour. Then the required similarity forms for solution of equations (2.8) are

$$\psi = \xi f(\eta), \quad \Delta = \xi^2 g(\eta) + k(\eta) \tag{2.14}$$

and f, g, k are universal functions to be determined.†

It should be noted that (2.14) satisfies the side-wall condition (2.10) automatically. In addition, note that (2.14) represents a truncation of a Taylor series expansion in ξ for ψ, Δ. At no other point may the Taylor series be truncated, incidentally. The form of (2.14) is essentially that used by Duncan (1966) for an axisymmetric solution.

Substitution of (2.14) into (2.8) gives

$$\left.\begin{aligned} f^{\mathrm{iv}} &= 2g + \frac{1}{\sigma}(f'f'' - ff'''), \\ g'' &= 2f'g - fg', \quad k'' = -fk', \end{aligned}\right\} \tag{2.15}$$

where the superscripts denote the order of differentiation with respect to η. The boundary conditions (2.9) become

$$f = 0, \quad f' = 0, \quad g = 1, \quad k = 0, \quad \text{at} \quad \eta = 0, \tag{2.16a–d}$$

as well as the requirement that the system be steady: namely that there is no net buoyancy flux into the box. Since all other surfaces are insulating,

$$\text{at} \quad \eta = 0, \quad Q_N \equiv \int_0^1 \frac{\partial \Delta}{\partial \eta} d\xi = 0.$$

From (2.14) this gives

$$\text{at} \quad \eta = 0, \quad k' = -\tfrac{1}{3}g'. \tag{2.16e}$$

The other boundary conditions are:

$$\text{case (i), as} \quad \eta \to \infty, \quad f \sim C, \quad g \sim 0; \tag{2.17a}$$

or

$$\text{case (ii), as} \quad \eta \to \infty, \quad f \sim A\eta + B, \quad g \sim 0. \tag{2.17b}$$

Thus the problem to be solved is (2.15) with boundary conditions (2.16) and either (2.17*a*) or (2.17*b*). Since the lower boundary layer must be thin, $\delta \ll H$, and the interior must be describable by (2.12), restrictions on the applicability of the solutions are that

$$\sigma > 1 \quad \text{and} \quad Ra_L \gg (L/H)^5 \gg 1. \tag{2.18}$$

(In what follows, σ is treated as an $O(1)$ quantity unless otherwise stated.)

3. Solutions and results

Numerical solutions were obtained with modified forms of (2.17) as boundary conditions. Precise forms of these will be discussed below. The Taylor system (Norman 1972) was used for the simulation of the equations.‡

† Note that a quadratic distribution of heat *flux* imposed on the lower boundary can also be handled with this formulation; the boundary layer scales with $Ra_L^{-\frac{1}{6}}$.

‡ This system automatically differentiates the equations many times, evaluates a Taylor series solution, and writes Fortran subroutines to solve the problem to the accuracy of the computer.

Consider case (i) first. As $\eta \to \infty$, (2.15) becomes

$$f^{\mathrm{iv}} \sim 2g - \frac{C}{\sigma} f''', \tag{3.1}$$

$$g'' \sim -Cg', \tag{3.2}$$

$$k'' \sim -Ck', \tag{3.3}$$

with asymptotic solution

$$g = g_0 e^{-C\eta}, \tag{3.4}$$

$$k = k_0 e^{-C\eta} + k_\infty, \tag{3.5}$$

$$f - C = \frac{2g_0}{C^4} e^{-C\eta} + \alpha e^{-C\eta/\sigma}, \tag{3.6}$$

for some unknown constants g_0, k_0, k_∞, α and C. It is clear that all five constants will be necessary to satisfy the five boundary conditions at $\eta = 0$. For $\sigma > 1$, the second term in (3.6) dominates the first. This means that the boundary layer splits into two. The thinner, inner layer is thermally driven, and is of width order unity or C^{-1}, whichever is larger; whereas the outer layer, of width σC^{-1}, is dynamically driven and is essentially homogeneous.

It is interesting that the nonlinear momentum terms are important in this solution; a scaling based on large σ would have rejected them (the resulting problem has no solution). However, they have virtually no influence on the thermal field.† The outer layer is very wide for large σ, but it is possible to avoid excessive integrations by employing the asymptotic solutions

$$g \sim g_0 e^{-f\eta}, \tag{3.7}$$

$$k \sim k_0 e^{-f\eta} + k_\infty, \tag{3.8}$$

$$f \sim C + \alpha e^{-C\eta/\sigma}, \tag{3.9}$$

at a value of η sufficiently large so that g is very small ($\eta = 6$ was chosen; with confirmation from larger values *a posteriori*). Starting from these asymptotics ((3.9) is an exact solution of (2.15*a*) with g set to zero), (2.15) are then integrated inwards to $\eta = 0$, and the five constants then adjusted to satisfy the boundary conditions (2.16).

The solution is shown in figure 2(*a*), for $\sigma = 5$ and $\sigma = 18$. It demonstrates the very weak dependence on σ for $\eta < 2$ (the thermally driven region), followed by the transition to the viscous-inertial balance for large η, which does vary with σ. The derivatives of f and g at $\eta = 0$, i.e. $f''(0)$, $f'''(0)$, $g'(0)$, vary by less than $\frac{1}{3}$%, 6% and 2·5% respectively as σ varies from 5 to 75, so that the thermal layer solution is approximately independent of σ. Similarly, k_∞ varies by less than 2%, being essentially determined in the inner layer. For $\eta \gtrsim 3$, the solution is approximately homogeneous: $g \sim 0$, $k \sim k_\infty$.

Figure 2(*b*) shows the variation of C with σ. The asymptotic value for large σ ($\geqslant 5$) is, for $\sigma < 100$,

$$C \sim 0{\cdot}86\sigma^{0{\cdot}48}, \tag{3.10}$$

† Attempts to use matched asymptotic expansion methods fail because the inner layer is still nonlinear and therefore not tractable.

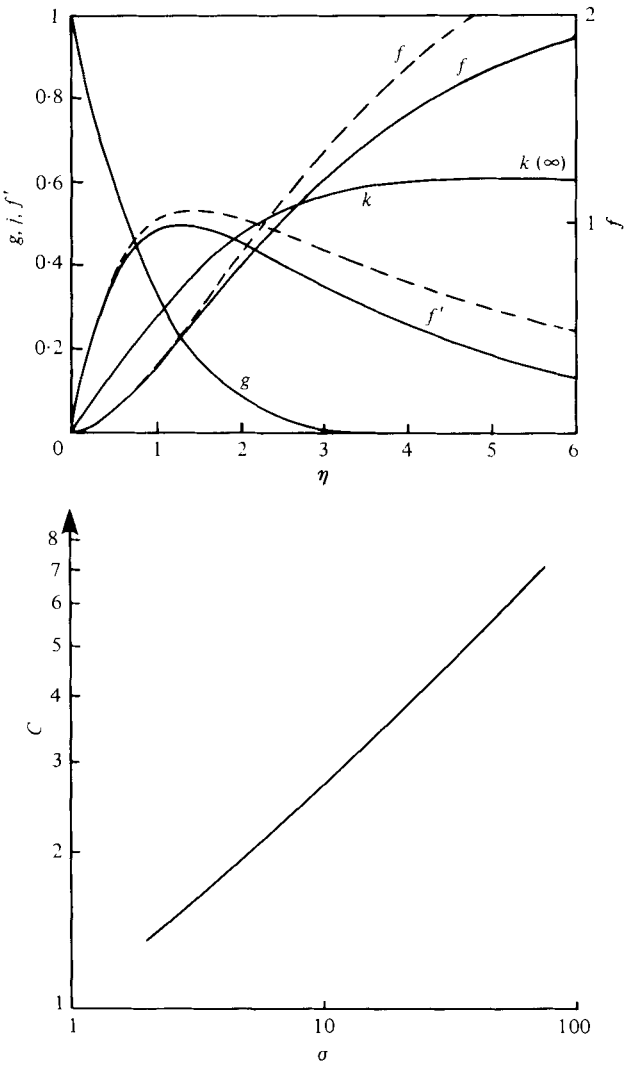

FIGURE 2. Similarity solutions for the lower boundary layer in figure 1 for the case of a laminar side-wall layer. (*a*) ——, $\sigma = 7$; – – –, $\sigma = 18$; g and k are so similar at $\sigma = 7$, 18 that only the former case is shown. (*b*) Variation of $C = f(\eta \to \infty)$ with σ.

so that a measure of the thickness of the outer layer, σC^{-1}, varies as $\sigma^{1-0\cdot48} = \sigma^{0\cdot52}$. The result (3.10) is in disagreement with the findings of Somerville (1967), and Beardsley & Festa (1972). Both found that the maximum interior stream function was insensitive to values of σ larger than about 10. The difference is due to the low values of Ra_L (less than 10^6) used in these studies. The non-dimensional width of the viscous inertial boundary layer is, from (2.5), (3.10),

$$(LH^{-1})\, Ra_L^{-\frac{1}{5}}\, \sigma^{0\cdot52},$$

which for a square cell is of order unity for $Ra_L = 10^5$, $\sigma \gtrsim 1$. Thus the outer layer overlaps the interior of the fluid, so that ψ cannot reach its full value, in their studies. Only when $Ra_L \gtrsim 10^8$ and σ moderate, can we expect the asymptotic solution to hold.

Case (ii), the turbulent plume, is more straightforward. As $\eta \to \infty$, (2.15) becomes

$$f^{\mathrm{iv}} \sim 2g + \frac{1}{\sigma}(Af'' - (A\eta + B)f'''), \tag{3.11}$$

$$g'' \sim 2Ag - (A\eta + B)g', \tag{3.12}$$

$$k'' \sim -(A\eta + B)k', \tag{3.13}$$

with asymptotic solution

$$k = k_0 \int_\infty^\eta \exp -(\tfrac{1}{2}A\eta^2 + B\eta)\, d\eta + k_\infty, \tag{3.14}$$

$$g = g_0\{(A\eta + B)^2 + A\} \int_\infty^\eta \frac{\exp -(\tfrac{1}{2}A\eta^2 + B\eta)}{(A\eta + B)^2 + A}\, d\eta, \tag{3.15}$$

$$f = 2\left(\int_\infty^\eta d\eta\right)^4 g + \alpha\left(\int_\infty^\eta d\eta\right)^2 (A\eta + B) \int_\infty^\eta \frac{\exp[(-1/\sigma)(\tfrac{1}{2}A\eta^2 + B\eta)]}{(A\eta + B)^2}\, d\eta, \tag{3.16}$$

where powers of integrals denote repeated integration. Equations (3.14)–(3.15) involve a total of six adjustable constants, whereas (2.11) give only five boundary conditions at $\eta = 0$. (The apparent degree of freedom in the problem is illusory, however.) As the asymptotics (3.14)–(3.16) are too complicated to use numerically, the alternative method of integrating outwards from $\eta = 0$ to a large value ($\eta = 10$) was employed, followed by imposing the approximate conditions

$$f'' = f''' = g = 0, \quad \eta = 10. \tag{3.17}$$

The guessed values of $f''(0)$, $f'''(0)$ and $g'(0)$ can then be adjusted to satisfy (3.17).

The solution is illustrated in figure 3(*a*), which shows clearly that f'' and g share the same decay scale; the coefficient α in (3.16) is in fact very small for $\sigma \gtrsim 5$. However, unlike case (i), a solution exists for σ infinite (with only five adjustable constants), and non-infinite σ merely presents an $O(\sigma^{-1})$ perturbation to the σ-infinite case. This perturbation is that which would be found in a straightforward expansion of the problem in powers of σ^{-1}, in fact.† The solution appears to be unique; a considerable amount of computer time was spent attempting to obtain other solutions with a variety of methods, all without success. (Indeed, uniqueness cannot be established even for the much simpler Falkner–Skan problem, see Batchelor (1967, chap. 5).) The buoyancy distribution is almost identical to case (i).

The effect of the nonlinear momentum terms is thus very weak for $\sigma \gtrsim 5$, say. Figure 3(*a*) shows that the boundary-layer behaviour has reached its asymptote in the interior for $\eta \gtrsim 3$, so that (3.17), for example, is adequate. Figure 3(*b*) shows how the asymptotic solutions vary with σ. The insensitivity with respect to σ is interesting, and must await experimental confirmation. Of particular note is that the asymptotic value of the buoyancy, k_∞, is again found to be independent of $\sigma > 1$ to within 0·4 %. Being typical of the results, the solution for infinite σ will be used in the following discussion whereas, in the laminar case, the solution for $\sigma = 7$ (heated water) will normally be used.

† The lack of such a solution in the laminar case is what gives rise to the double-layer structure.

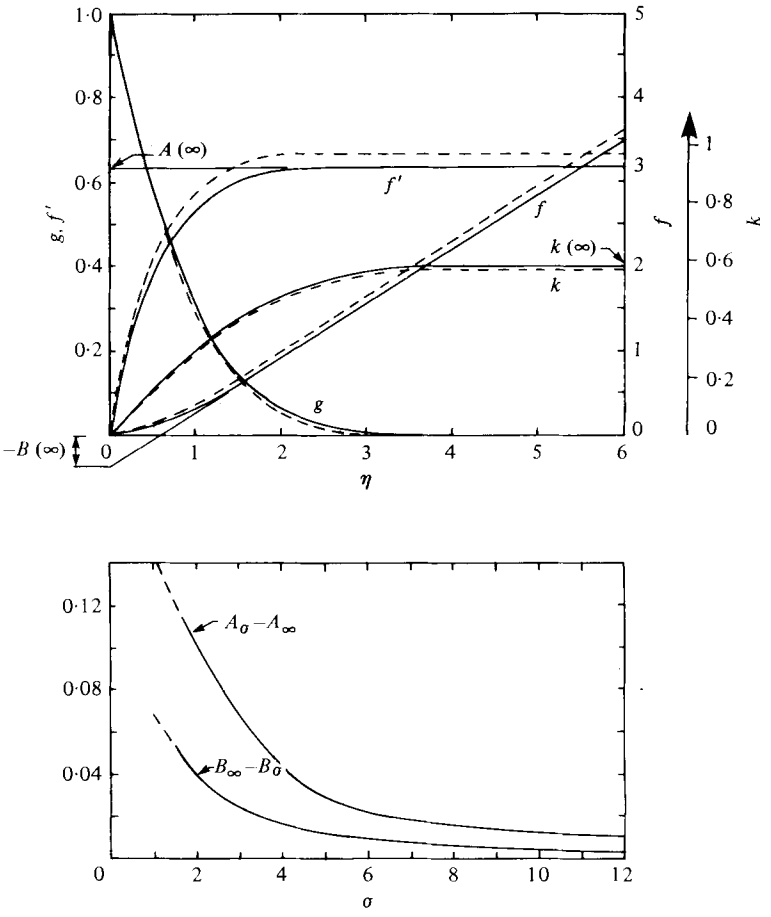

FIGURE 3. Similarity solutions for the lower boundary layer in figure 1 for the case of a turbulent side-wall plume. (*a*) ——, $\sigma = \infty$; – – –, $\sigma = 5$. (*b*) Variations of A, B as functions of σ.

Case (i) can be connected with case (ii) very simply, when σ is large, by means of matched asymptotic expansions. Consider $\eta \sim O(1)$ to be the inner region, where the nonlinear momentum terms are negligible. Let the outer region be characterized, for large σ, by

$$Y = \sigma^b \eta, \quad f = \sigma^a F, \quad \Delta = \Delta_I, \quad a, b > 0, \tag{3.18}$$

where a, b are to be found. Substitution in (2.15) yields

$$a + b = 1 \tag{3.19}$$

and

$$F = a + b\, e^{-aY}. \tag{3.20}$$

Matching between inner and outer regions involves, essentially, equality of f and its derivatives between the inner solution as $\eta \to \infty$ and the outer as $Y \to 0$. The inner solution can only be that for case (ii), the turbulent plume, since no inner solution exists with $f \to$ constant. Hence

$$a = b = \tfrac{1}{2}, \quad F(0) = 0, \quad F_Y(0) = f'(\eta \to \infty) = \frac{d}{d\eta}(A\eta + B) = A; \tag{3.21}$$

and higher derivatives are trivially continuous to leading order. Thus

$$F = a(1 - e^{-aY}) \tag{3.22}$$

and

$$a = A^{\frac{1}{2}}. \tag{3.23}$$

From § 4, $a \sim 0{\cdot}80$, so that

$$C = f(\eta \to \infty) \sim 0{\cdot}80\sigma^{\frac{1}{2}}, \tag{3.24}$$

which is in excellent agreement with (3.10), over the range studied. Thus the strong agreement between buoyancy distributions in cases (i) and (ii) is now explained.

It is easy to see that the double-layer structure is a general feature of the problem, and not just of the similarity solution. One can see physically why there must be two layers. There is interior downwelling, which impinges on the bottom, no-slip boundary. Were there no stratification, the downwelling would be turned by a balance between nonlinear and viscous vorticity terms. The existence of stratification cannot completely remove this layer because there is insufficient freedom in the buoyancy layer to satisfy all the boundary conditions.

4. Interior asymptotes

The asymptotes for case (i) for large η are computed to be

$$f \sim 0{\cdot}86\sigma^{0{\cdot}48} (\sim 2{\cdot}29 \quad \text{for} \quad \sigma = 7), \quad g \sim 0, \quad k \sim 0{\cdot}60. \tag{4.1}$$

Similarly, for case (ii)

$$f \sim 0{\cdot}638\eta - 0{\cdot}34, \quad g \sim 0, \quad k \sim 0{\cdot}58. \tag{4.2}$$

(Note the similarity of the two k values.)

We can estimate when case (ii) is relevant instead of case (i) for increasing Ra_L by assuming a critical Reynolds number for turbulence and hence entrainment of interior fluid by the plume. Now from (4.1),

$$Re \equiv \frac{u'\delta}{\nu} = \frac{\kappa}{\nu} Ra_L^{\frac{1}{4}} \psi \sim \frac{2{\cdot}29 Ra_L^{\frac{1}{4}}}{\sigma}.$$

If the critical value of Re is 10^3, $Ra_L \simeq (440\sigma)^5$ delimits case (i) from case (ii). With $\sigma = 7$, case (i) is relevant for $Ra_L < 3 \times 10^{17}$; a turbulent plume requires an exceptionally large Rayleigh number!†

Comparison of the present model with past work is now possible. Case (i) is applicable since the maximum Rayleigh number reported is $1{\cdot}6 \times 10^{10}$ (Rossby 1965). Rossby estimated a value for the interior buoyancy to be 70 % of the maximum imposed at the bottom of his experimental cell, and this value was found to be substantially independent of Rayleigh number in the range 10^7 to 10^{10}. The numerical experiments of Beardsley & Festa (1972) support a somewhat lower value but this may be attributable to the lower Rayleigh numbers studied and the use of a free-slip boundary condition (see appendix B for a discussion of this problem). Now from (4.1) the

† The non-turbulent Ra_L would not be, then, a relevant characterizing group for the model, and a turbulent value of Ra_L would be needed; cf. a turbulent Re of order unity for fully turbulent flow, where the mean flow Re could be very large.

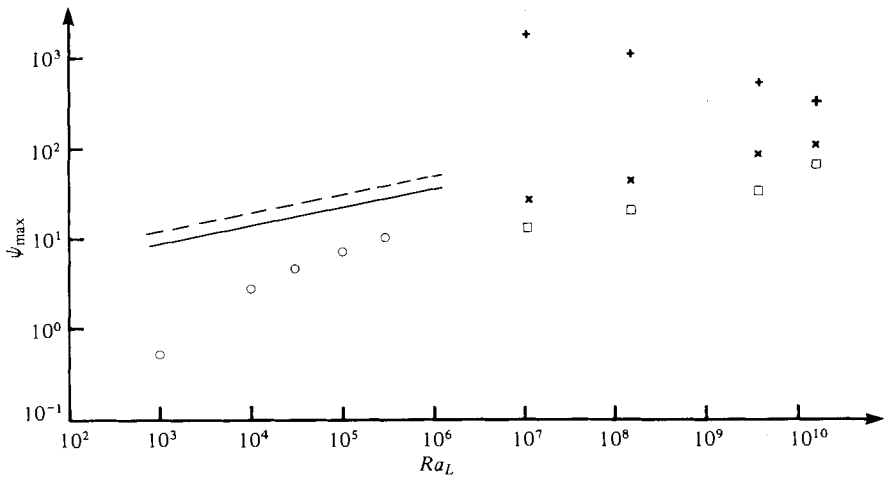

FIGURE 4. Non-dimensional maximum stream function ($= \psi'_{max}/\kappa$) as a function of Ra_L. The left-hand side shows Beardsley & Festa's (1972) experiments (○), and the predictions of the model for rigid (——) and free-slip (– – –) boundaries. The right-hand side shows Rossby's (1965) experimental results (□), together with the present theoretical predictions (+), and the present predictions calculated the same way as Rossby (×). Note that the predictions for ψ_{max} decrease with Ra_L because of the Prandtl-number dependence.

asymptote of k predicts the interior buoyancy to be 60% of maximum imposed, independent of Rayleigh number, which is consistent with Rossby's results and also with the fact that the greater non-uniformity of a quadratic impressed buoyancy probably results in a lower interior value. Since the interior is advectively warmed, its temperature is an average of the warm fluid supplying it. Note that this conflicts with Stern's (1975) assumption that abyssal temperature is approximately that of the hottest fluid on the boundary.

The greater non-uniformity of the impressed buoyancy field also probably explains the stronger circulation predicted for the quadratic as compared with a linear distribution. (The wide boundary-layer width for $Ra_L \sim 10^5$, noted previously, also plays a part in the explanation.) Figure 4 compares the maximum dimensionless stream function, predicted from (3.10), using (2.5), to be

$$\psi_{max} \equiv \psi'(\eta \to \infty)/\kappa = 0{\cdot}86\sigma^{0{\cdot}48} Ra_L^{\frac{1}{4}}$$

with results of Rossby and Beardsley & Festa. (The latter paper used free-slip conditions, in fact; results from appendix B are plotted as the dashed line for comparison.) Noting that the aspect ratio, L/H, in Rossby's experiments was 2·5, and that, from (2.18), $Ra_L \gg 100$ for the model to be valid, we see that the trends are in good agreement with Beardsley & Festa (not with Rossby) but that the quadratic impressed field results in a circulation some four times stronger than observed for a linear field. A greater acceleration is imparted to the fluid in the lower boundary layer by the increasing buoyancy gradient with distance along the bottom, by equation (2.8a).

The total disagreement with Rossby's data is at first discouraging. However, Rossby estimated ψ_{max} from $u'_{max}\,\hat{\delta}$, where u'_{max} was the maximum horizontal velocity observed, and $\hat{\delta}$ an estimate of boundary-layer thickness. It is easy to see from figure 2 that such a calculation on our model would yield estimates of ψ_{max} *much* smaller

than C. For comparison, then, $\hat{\psi}_{\max}$ has been computed from the model as $Ra_L^{\frac{1}{5}} u_{\max} \tilde{\delta}$, where now $\tilde{\delta}$ is the value of η at which Δ_ξ reduces to one-tenth its value at $\eta = 0$ (i.e. $\tilde{\delta} \approx 1{\cdot}8$). Figure 4 shows that $\hat{\psi}_{\max}$ differs by only a factor of 2 from Rossby's (non-dimensional) estimates, which, given the error sources in the experiment, and the different boundary conditions, appears quite good agreement with data.

Case (ii) permits prediction at very large Rayleigh numbers. From (4.2), the interior buoyancy is much the same as before, being 58 % of maximum impressed. The interior asymptote for the stream function is (from (2.5), (2.12))

$$\begin{aligned} \psi_I' &\sim 0{\cdot}638\kappa\, Ra_L^{\frac{1}{5}}\, \xi(\eta - 0{\cdot}53) \\ &\sim 0{\cdot}638\kappa \frac{H}{L} Ra_L^{\frac{2}{5}}\, \xi\left(\zeta - 0{\cdot}53 \Big/ \left(\frac{H}{L} Ra_L^{\frac{1}{5}}\right)\right). \end{aligned} \tag{4.3}$$

Thus the virtual origin of the plume insofar as it affects the interior, ζ_0, is

$$\zeta_0 = 0{\cdot}53 \frac{L}{H} Ra_L^{-\frac{1}{5}} = 0{\cdot}52 \frac{\delta}{H}. \tag{4.4}$$

That is, the plume appears to originate within the boundary layer, supporting the form ψ_I' used here. Further, (4.3) shows that, for a fixed level within the cell, ψ_I' is predicted to be proportional to $Ra_L^{\frac{2}{5}}$ and inversely proportional to the aspect ratio L/H. This compares with $\psi_I' \sim C\kappa\, Ra_L^{\frac{1}{5}}$ for case (i), at lower values of Ra_L.

5. Flux exchange with environment

So as to maintain a steady state, a particle displaced from the (almost) isothermal interior into the lower boundary layer is first cooled and then warmed by exchange with the lower boundary as it accelerates toward the right-hand side of the cell. Figure 5(*a*) illustrates the buoyancy distribution in the layer obtained by plotting (2.14*b*) for case (i) (case (ii) is almost identical and is not shown). The similarity of the field with that found by Rossby (1965), the numerical models, and Hignett (1979), reproduced in figure 5(*b*), is striking (recall that the right-hand side-wall layer is omitted; there the flow turns upwards into the interior, as a narrow jet).

Plotted in figure 6 is the vertical buoyancy gradient $-\partial\Delta/\partial\eta$ at the lower boundary (cases (i) and (ii) are indistinguishable) together with the result if heat transfer in the cell were achieved solely by heat conduction. In that case the problem is to solve

$$\nabla^2 \Delta' = 0$$

such that

$$\frac{\partial \Delta}{\partial \xi} = 0 \quad \text{on} \quad \xi = 0, 1,$$

$$\frac{\partial \Delta}{\partial \zeta} = 0 \quad \text{on} \quad \zeta = 1$$

and

$$\Delta = \xi^2 \quad \text{on} \quad \zeta = 0.$$

The solution is

$$\Delta = \tfrac{1}{3} + \sum_{n=1}^{\infty} \frac{4(-1)^n}{(n\pi)^2} \cos n\pi\xi \frac{\cosh\left(n\pi/D\right)(\zeta - 1)}{\cosh\left(n\pi/D\right)}$$

so

$$\text{at} \quad \zeta = 0, \quad \left.\frac{\partial \Delta}{\partial \zeta}\right|_{\text{conduction}} = \sum_{n=1}^{\infty} \frac{4(-1)^{n-1}}{n\pi D} \cos n\pi\xi \tanh \frac{n\pi}{D}, \tag{5.1}$$

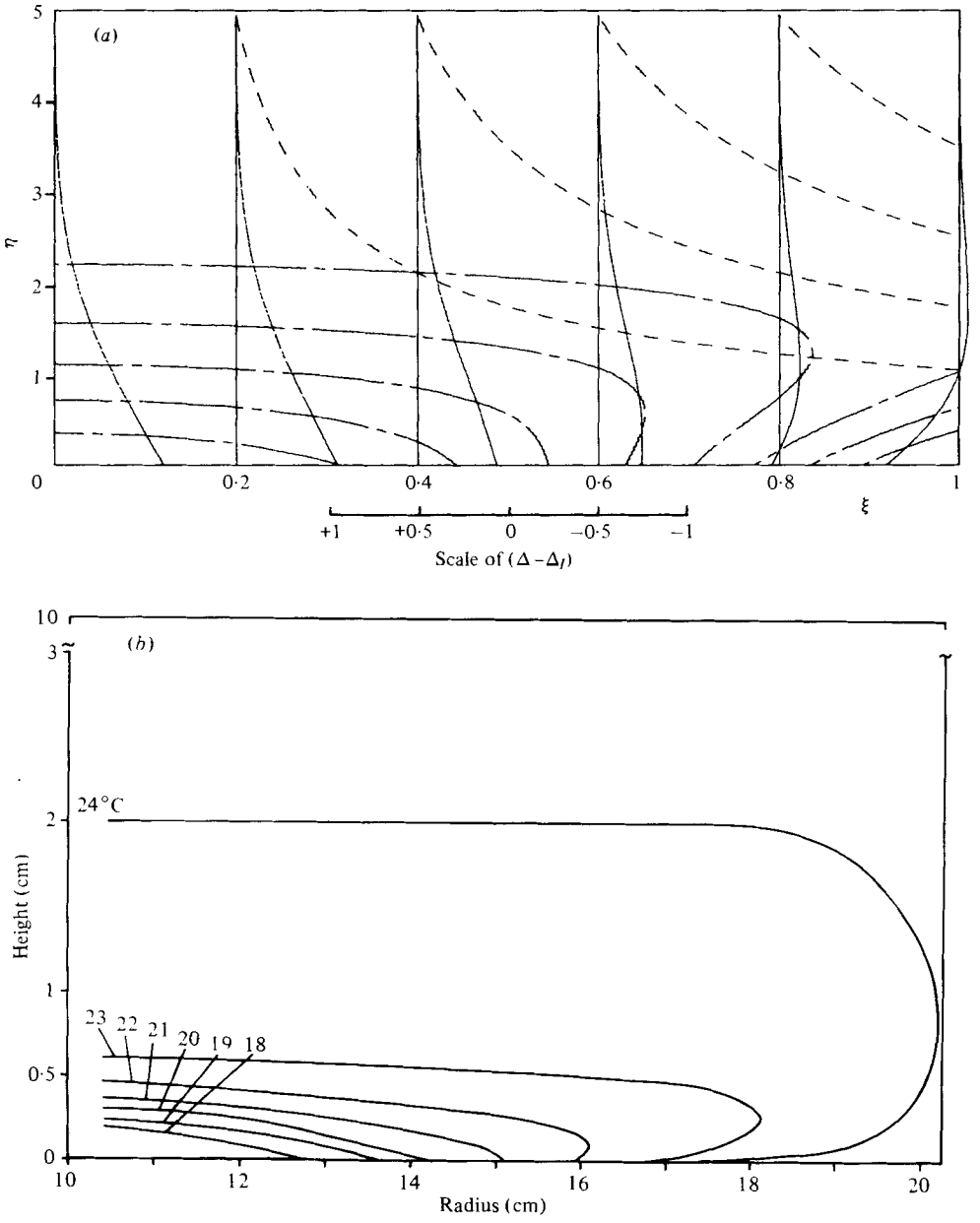

FIGURE 5. (*a*) Plot relative to the interior of the computed buoyancy distribution in the vicinity of the lower boundary at equidistant vertical sections for $\sigma = 7$ and a laminar plume. The results for a turbulent plume are almost identical. The chain lines (— — —) are equally-spaced isopycnals. The dashed lines (– – –) are equally-spaced streamlines, which are then returned upwards in the side-wall layer on $\xi = 1$. (*b*) Contours of temperature found experimentally by Hignett (1979) in an annulus approximately 10 × 10 cm. The imposed temperature is not quadratic, and varies from 12·6 °C to 27·8 °C. The fluid is water, with $Ra_L = 2 \times 10^8$.

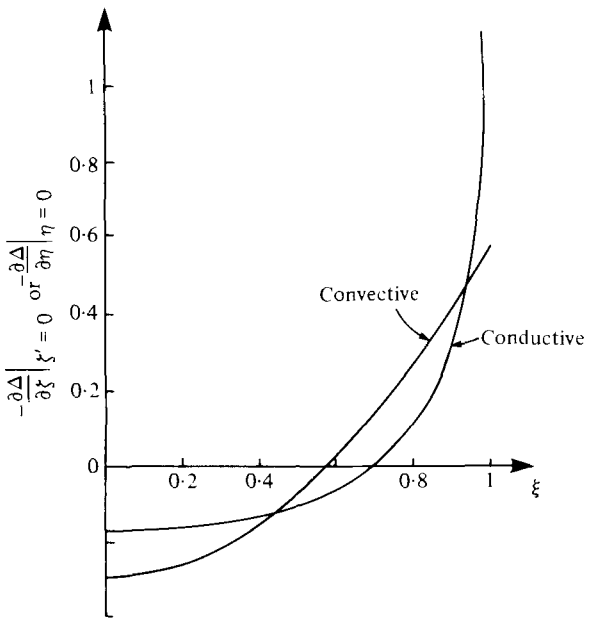

FIGURE 6. The non-dimensional buoyancy gradient $-\partial\Delta/\partial\eta$ on $\eta = 0$ as a function of ξ, from (2.14). Also shown is $-\partial\Delta/\partial\zeta$ on $\zeta = 0$ in the case of pure conduction, from (5.1). The aspect ratio $D = LH^{-1}$ is 2·5.

where $D = L/H$ is the aspect ratio. Convection in the box reduces the extreme warming in the vicinity of the plume origin, spreading this phase over a greater length of the boundary, as shown in figure 6.

Following Rossby (1965), define a Nusselt number based on the gross buoyancy flux into the box, Q_G, by $Nu_G = Q_G/Q_{G\,\text{conduction}}$. Now

$$Q_G = \tfrac{1}{2}\kappa \int_0^L \left|\frac{\partial\Delta'}{\partial z}\right|_{z=0} dx.$$

From (2.14*b*) and (2.16*c*), $\partial\Delta/\partial\eta = 0$ at $\eta = 0$, $\xi = 1/\sqrt{3}$ so that

$$Q_G = \frac{-2}{9\sqrt{3}} g'(0)\,\kappa\Delta_m\, Ra_L^{\frac{1}{2}}, \tag{5.2}$$

and for case (i), $g'(0) = -0{\cdot}85$ (for case (ii), $g'(0) = -0{\cdot}87$). From (5.1)

$$Q_{G\,\text{conduction}} = \tfrac{1}{2}\kappa\Delta_m \int_0^1 \left| \sum_{n=1}^{\infty} \frac{4(-1)^{n-1}}{n\pi} \cos n\pi\xi \tanh\frac{n\pi}{D} \right| d\xi. \tag{5.3}$$

Relation (5.3) is approximately independent of aspect ratio near $D = 1$ but ultimately decreases like $1/D$ for large D. For $D = 2{\cdot}5$ (Rossby's experiments),

$$Q_{G\,\text{conduction}} \approx 0{\cdot}360\kappa\Delta_m$$

so

$$\text{for} \quad D = 2{\cdot}5, \quad Nu_G = 0{\cdot}30 Ra_L^{\frac{1}{3}}; \tag{5.4}$$

$$\text{for} \quad D = 1{\cdot}0, \quad Nu_G = 0{\cdot}26 Ra_L^{\frac{1}{3}}. \tag{5.5}$$

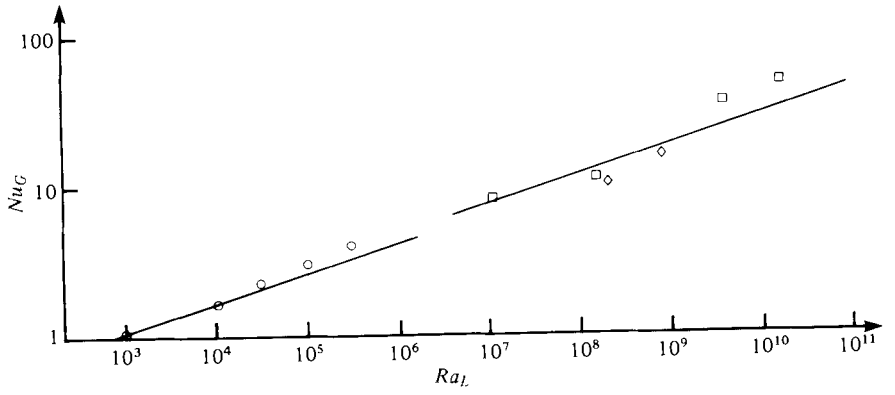

FIGURE 7. The Nusselt number Nu_G as a function of Rayleigh number Ra_L. ○, Beardsley & Festa's (1972) results ($D = 1{\cdot}0$); □, Rossby's (1965) results ($D = 2{\cdot}5$); ◇, two results of Hignett (private communication) ($D = 1{\cdot}0$). The straight lines show the theoretical prediction.

Figure 7 illustrates Rossby's (1965) results for Nu_G compared with (5.4). It also shows Beardsley & Festa's (1972) results (obtained for a square cell) compared with (5.5), together with measurements by Hignett (private communication), also for a square cell. The agreement is excellent in view of the differing boundary conditions. The independence from Prandtl number as suggested by (5.4), (5.5), is confirmed, and the weak dependence on aspect ratio is also supported.

6. Discussion

By imposing a quadratic temperature distribution on the bottom of the otherwise insulated rectangular two-dimensional cell and imposing conditions of no-slip on this boundary, we have been able to obtain similarity solutions for the boundary layer and interior for the problem first posed by Stommel (1962). The utilization of interior forms for ψ and Δ indicated by a previous study of a discrete plume in a box (Manins 1979) and the recognition that the plume and outflow merely provide consistency conditions in the laminar case, and are of secondary importance in the turbulent case, has been central to the approach.

The interior buoyancy and gross Nusselt number have been shown to be insensitive to Prandtl number ($\sigma > 1$) and to be primarily functions of the horizontal Rayleigh number Ra_L. The interior stream function varies roughly as the square root of the Prandtl number in the laminar case, and is insensitive to it in the turbulent case. In either case, values of stream function within the *thermal* boundary layer are quite insensitive to Prandtl number. In view of the differing boundary conditions, the agreement with Rossby's (1965) laboratory results and the numerical results of Beardsley & Festa (1972) is satisfactory.

Some useful conclusions may be drawn from this study regarding the efficiency of the exchange of buoyancy of the archetypal system with the environment: the dynamics of the side-wall plume are not important in determining the character of the circulation nor the interior buoyancy. Details of the shape of the impressed buoyancy field on the lower diabatic boundary appear to be unimportant so far as the overall

buoyancy exchange as measured by a gross Nusselt number is concerned. Indeed, a description of the diabatic layer (primarily in terms of horizontal Rayleigh number) is sufficient to provide an accurate determination of efficiency.

This paper originated from work by the second author while at Cambridge (Manins 1973). He thanks A. E. Gill for suggesting Rossby's paper for study and J. S. Turner for inspiration and example. The first author would like to thank P. Hignett and A. Ibbetson for laboratory results in rotating and non-rotating annuli which gave this paper its final stimulation.

Appendix A. The side-wall boundary layers in the laminar regime

(*a*) *The cold wall*

Integrating the non-dimensional form of (2.3*b*) between $\zeta = 0$ and 1, and from $\xi = 0$ to ξ yields

$$Ra_L^{\frac{1}{5}} D^{-1} \int_0^1 \psi_\zeta (\Delta - \Delta_I)\, d\zeta = -\int_0^\xi \Delta_\zeta \Big|_{\zeta=0} d\xi, \tag{A 1}$$

where D is the aspect ratio LH^{-1}. Thus, following Stern (1975),

$$\int_0^1 \psi_\zeta (\Delta - \Delta_I)\, d\zeta = -\int_0^1 \psi \Delta_\zeta \, d\zeta \to 0, \quad \xi \to 0 \text{ or } 1. \tag{A 2}$$

On the cold wall ($\xi = 0$), Δ_ζ is one-signed, as the fluid has its maximum density on $\xi = \zeta = 0$. Since ψ cannot change sign (this would involve flow *towards* the cold wall), (A 2) implies that

$$\psi = 0, \quad \xi \to 0 \tag{A 3}$$

is the relevant condition on the interior stream function. Equation (2.8*a*) then implies that $\Delta_\xi = 0$, $\xi \to 0$ is also satisfied. Hence only the no-slip condition on $\xi = 0$ remains to be satisfied. This is achieved by a boundary layer of thickness $Ra_L^{-\frac{3}{10}}$ (and still of depth $Ra_L^{-\frac{1}{5}}$, i.e. within the bottom boundary layer). The dynamics are similar to those found by Walin (1971). Let

$$\psi \doteq Ra_L^{-\frac{3}{10}} \psi_1 \left(X = \frac{\xi}{Ra_L^{-\frac{3}{10}}}, \eta \right) + \xi \psi_{B\xi}, \tag{A 4}$$

$$\Delta \doteq Ra_L^{-\frac{1}{5}} \Delta_1(X, \eta) + \Delta_B(\eta), \tag{A 5}$$

near $\xi = 0$, where the vanishing of ψ and Δ_ξ in the bottom layer (suffix B) has been allowed for. ψ_1, Δ_1 vanish as $X \to \infty$. Then (2.6) become

$$\psi_{1XXXX} = \Delta_{1X}, \tag{A 6}$$

$$\Delta_{1XX} = -\psi_{1X} \Delta_{B\eta}, \tag{A 7}$$

or

$$\Delta_{1XXXX} = -\Delta_{B\eta} \Delta_1. \tag{A 8}$$

Since

$$\Delta_{B\eta} > 0 \tag{A 9}$$

(A 8) has 2 roots which decay for large positive X and, to satisfy the boundary conditions

$$\Delta_{1X} = 0, \quad \psi_{1X} = -\psi_{B\xi}, \quad X = 0 \tag{A 10}$$

(which makes $\psi_1 = 0$ also, incidentally), the solution is

$$\psi_1 = \frac{-2^{\frac{1}{2}}}{(\Delta_{B\eta})^{\frac{1}{4}}} \psi_{B\xi} \exp\left(\frac{-\Delta_{B\eta}^{\frac{1}{4}}}{2^{\frac{1}{2}}} X\right) \sin \frac{\Delta_{B\eta}^{\frac{1}{4}}}{2^{\frac{1}{2}}} X, \tag{A 11}$$

$$\Delta_1 = -\Delta_{B\eta}^{\frac{1}{2}} \psi_{B\xi} \exp\left(\frac{-\Delta_{B\eta}^{\frac{1}{4}}}{2^{\frac{1}{2}}} X\right) \left(\sin \frac{\Delta_{B\eta}^{\frac{1}{4}}}{2^{\frac{1}{2}}} X + \cos \frac{\Delta_{B\eta}^{\frac{1}{4}}}{2^{\frac{1}{2}}} X\right). \tag{A 12}$$

(*b*) *The hot wall*

Equation (A 2) still holds as $\xi \to 1$, but now Δ_η (or Δ_ζ) changes sign with η: Δ_B is less dense than the interior, but above the base there is fluid which is more dense than the interior. Since ψ cannot be zero on $\xi = 1$ (which would imply that w changes sign with ξ somewhere in the interior), (A 2) yields no useful consistency condition on the interior flow. Indeed, no consistency condition has been found, owing to the non-linearity of the side-wall layers.

The structure of the side-wall layers is of interest, and will be briefly described. A useful constraint is found from a direct integration of the non-dimensional form of (2.3*b*):

$$\int_0^1 d\xi \, (\Delta_\zeta + Ra_L^{\frac{1}{4}} \psi_\xi \Delta) = 0, \tag{A 13}$$

where the aspect ratio D has been set to unity. This states that the *total* vertical buoyancy transfer (by diffusion and advection) at any level must vanish.

Away from the bottom layer (i.e. where ζ is order unity) the contribution of Δ_ζ to (A 13) is zero, or at least exponentially small. Since Δ is homogeneous (i.e. $= \Delta_I$) in the interior, the vertical advection term may be written

$$Ra_L^{\frac{1}{4}} \left\{ \int_0^1 d\xi \, \psi_\xi \Delta_I + \int_0^1 d\xi \, \psi_\xi (\Delta - \Delta_I) \right\}$$

and the first term vanishes because of the boundary condition on ψ. Hence (A 13) requires there to be no anomalous vertical buoyancy transport in any side-wall layer, or

$$\int_0^1 d\xi \, \psi_\xi (\Delta - \Delta_I) = 0. \tag{A 14}$$

Now the scaling for a side-wall layer far from the bottom boundary must be (Rossby 1965)

$$\psi \sim \psi_i(\xi, \zeta) + \psi_1\left(X = \frac{\xi - 1}{Ra_L^{-\frac{1}{5}}}, \zeta\right), \tag{A 15}$$

$$\Delta \sim \Delta_I + Ra_L^{-\frac{1}{5}} \Delta_1(X, \zeta), \tag{A 16}$$

where suffix i denotes the solution far from the side-wall layer. ψ_1 and Δ_1 vanish as $X \to -\infty$. Equations (2.3) then become

$$\psi_{1XXXX} = \Delta_{1X} - \frac{1}{\sigma} \{\psi_{1X} \psi_{1XX\zeta} - \psi_{i\zeta} \psi_{1XXX} - \psi_{1\zeta} \psi_{1XXX}\}, \tag{A 17}$$

$$\Delta_{1XX} = -\psi_{1X} \Delta_{1\zeta} + \Delta_{1X} (\psi_{i\zeta} + \psi_{1\zeta}). \tag{A 18}$$

Equation (A 17) may be integrated with respect to X once, but both (A 17) and (A 18) are fully nonlinear. As $X \to -\infty$, they become

$$\psi_{1XXX} = \Delta_1 + \frac{1}{\sigma}\psi_{i\zeta}\psi_{1XX}, \tag{A 19}$$

$$\Delta_{1X} = \psi_{i\zeta}\Delta_1, \tag{A 20}$$

which possess decaying solutions provided $u_i = \psi_{i\zeta}$ is positive, i.e. the flow is towards the wall. The layer thus represents a balance between outward diffusion and inward advection of vorticity, modified by buoyancy forces.

The vertical transport of buoyancy in this layer is proportional to

$$-\int_{-\infty}^{0} \psi_{1X}\Delta_1\,dX = \int_{-\infty}^{0} \psi_{1XX}^2\,dX - \frac{1}{\sigma}\frac{d}{d\zeta}\left(\frac{1}{2}\int_{-\infty}^{0}\psi_{1X}^3\,dX\right), \tag{A 21}$$

after some algebra. From (A 14), this must vanish. If σ is $O(1)$, as assumed implicitly, this presents no problems. But as σ increases, the first term on the right-hand side of (A 21) begins to dominate (except over a limited distance in ζ near the bottom). For large σ, then, ψ_1 must vanish and there is apparently no layer of this type.

What in fact occurs is that the width of the layer becomes formally $\sigma^{\frac{1}{2}}Ra_L^{-\frac{1}{4}}$ rather than $Ra_L^{-\frac{1}{4}}$, with a balance between nonlinear and viscous forces (rather like the stagnation flow problem; Batchelor (1967, pp. 285–289)), and simple advection of buoyancy. The uniform interior buoyancy thus implies that there is uniform buoyancy in the side-wall layer as well.† However, without knowing the distribution of $u_i(\zeta)$, the side-wall layer cannot be solved explicitly.

The dynamics of the turning region ($\eta \sim O(1)$, $\xi \approx 1$) are fairly similar. Its width is formally $Ra_L^{-\frac{2}{5}}$. Writing

$$\psi \sim \psi_B(\xi,\eta) + \psi_1\left(X = \frac{\xi - 1}{Ra_L^{-\frac{2}{5}}}, \eta\right), \tag{A 22}$$

$$\Delta \sim \Delta_B(\xi,\eta) + \Delta_1(X,\eta), \tag{A 23}$$

where suffix B now represents values in the bottom layer, (2.6) yields, after one integration,

$$\psi_{1X}(\Delta_{B\eta} + \Delta_{1\eta}) - \Delta_{1X}(\psi_{B\eta} + \psi_{1\eta}) + \Delta_{1XX} = 0, \tag{A 24}$$

$$\psi_{1XXX} = \frac{1}{\sigma}\{(\psi_{B\eta} + \psi_{1\eta})\psi_{1XX} - \psi_{1X}\psi_{1X\eta}\}, \tag{A 25}$$

so that the fluid turns the corner without feeling any buoyancy force, under a balance between nonlinear and viscous effects. The buoyancy is advected and diffused by the velocity field given by (A 25); Δ_1 tends to zero as η increases, as the fluid becomes homogeneous in the interior. The width of the layer (which is proportional to $\psi_{B\eta}^{-1}$) increases as η becomes large, eventually becoming the interior side-wall layer (A 17).

As σ becomes large, the structure of the turning region becomes more complicated. For $O(1)$ values of η, the layer width is $\sigma Ra_L^{-\frac{2}{5}}$. Within this turning region, the buoyancy

† Rossby's (1965) results for $\sigma = 13$ (which *do* show a non-uniform buoyancy in the side-wall layer) may perhaps have been caused by imperfect insulation. Only a tiny heat flux through the wall is needed to maintain a diffusive boundary layer.

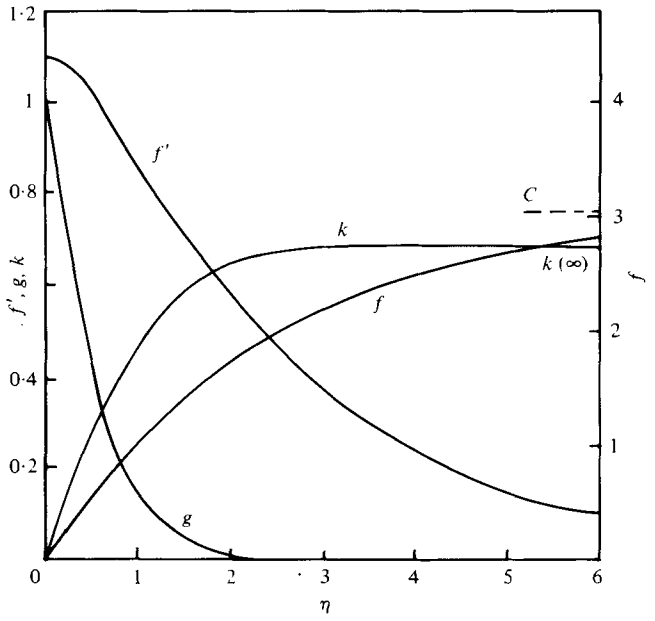

FIGURE 8. Similarity solutions for the lower boundary layer in figure 1 for the case of a laminar side-wall layer and free-slip bottom boundary, $\sigma = 7$.

equation is purely *advective*, together with a balance of nonlinear and viscous vorticity terms. This layer turns the fluid around the corner and upwards, in the direction of increasing η.

When η becomes of order $\sigma^{\frac{1}{4}}$, $\psi_{B\eta}$ is $O(1)$ and the layer width remains $\sigma Ra_L^{-\frac{2}{5}}$ (it will begin to widen as η increases further, until it matches onto the interior side-wall layer). The buoyancy balance remains advective.

It is clear that diffusion must become important somewhere, as otherwise buoyancy, conserved on streamlines, could not asymptote to the interior value Δ_I; in fact, the diffusion terms enter for η of order $\sigma^{\frac{1}{4}}$, in an inner layer of width $Ra_L^{-\frac{2}{5}}$, driven by the outflow from the turning region immediately beneath. This layer completes the specification of the side-wall boundary layers.

Appendix B. Free-slip boundary conditions

The numerical solutions of Somerville (1967) and Beardsley & Festa (1972) allowed free-slip conditions on the bottom boundary rather than rigid walls. This is simulated in our model by replacing (2.16*b*) by

$$f'' = 0, \quad \eta = 0. \tag{B 1}$$

The solution for case (i) (laminar plume) is shown in figure 8, for $\sigma = 7$. Comparison with figure 2 shows that the boundary layer is considerably thinner than in the no-slip case (Δ_ξ reaches $\frac{1}{10}$ its value at $\eta = 0$ when $\eta = 1{\cdot}2$; cf. 1.8 in the no-slip case). The horizontal velocity, f', is maximized at $\eta = 0$. The asymptotic buoyancy, k_∞, is increased to 0·68. Now Beardsley & Festa found the interior buoyancy to be

independent of the details of the velocity condition on the bottom boundary (although this was deduced from comparison of their free-slip computations and Rossby's experimental no-slip results).

Our results, however, would suggest an increase in Δ_I by 13 % when the condition is changed from no-slip to free-slip. (This seems quite plausible: the more rapid motion permitted in the lower layer with free-slip can advect more warm water into the interior.) The discrepancy may be again due to the rather wide bottom boundary layer in Beardsley & Festa's results, caused by their low values of Ra_L.

The constant C again varies with Prandtl number:

$$C \sim 1{\cdot}06\sigma^{0{\cdot}54} \tag{B 2}$$

(over a wide range of σ this would again vary as $\sigma^{\frac{1}{2}}$) so that the interior stream function (and therefore the vertical velocity) is stronger than in the no-slip case; again, this seems intuitive.

It should be noted, finally, that the solution for case (ii) (turbulent plume) is non-unique under free-slip conditions; there are an infinity of solutions possible, and the appropriate solution can only be determined by more detailed analysis of the plume itself.

REFERENCES

BATCHELOR, G. K. 1967 *An Introduction to Fluid Dynamics*. Cambridge University Press.

BEARDSLEY, R. C. & FESTA, J. F. 1972 A numerical model of convection driven by a surface stress and non-uniform horizontal heating. *J. Phys. Oceanog.* **2**, 444–455.

DUNCAN, I. B. 1966 Axisymmetric convection between two rotating disks. *J. Fluid Mech.* **24**, 417–449.

GOODY, R. M. & ROBINSON, A. R. 1966 A discussion of the deep circulation of the atmosphere of Venus. *Astrophys. J.* **146**, 339–355.

GOLDSTEIN, S. 1965 *Modern Developments in Fluid Dynamics*, vol. 1. Dover.

HIGNETT, P. 1979 Experiments on thermal convection in a rotating fluid annulus, driven by non-uniform heating from below. Ph.D. dissertation, University of Reading.

MCKENZIE, D. P., ROBERTS, J. M. & WEISS, N. O. 1973 Convection in the earth's mantle: towards a numerical simulation. *J. Fluid Mech.* **62**, 465–538.

MANINS, P. C. 1973 Confined convective flows. Ph.D. dissertation. University of Cambridge.

MANINS, P. C. 1979 Turbulent buoyant convection from a source in a confined region. *J. Fluid Mech.* **91**, 773–800.

NORMAN, A. C. 1972 A system for the solution of initial and two-point boundary value problems. *Proc. Ass. Comp. Mach.* (*25th Anniv. Conf., Boston*), pp. 826–834.

ROSSBY, H. T. 1965 On thermal convection driven by non-uniform heating from below: an experimental study. *Deep-Sea Res.* **12**, 9–16.

SOMERVILLE, R. C. J. 1967 A non-linear spectral model of convection in a fluid unevenly heated from below. *J. Atmos. Sci.* **24**, 665–676.

STERN, M. E. 1975 *Ocean Circulation Physics*. Academic.

STOMMEL, H. 1950 An example of thermal convection. *Trans. Am. Geophys. Union* **31**, 553–554.

STOMMEL, H. 1962 On the smallness of sinking regions in the ocean. *Proc. Natn. Acad. Sci.* **48**, 766–772.

STONE, P. H. 1968 Some properties of Hadley regimes on rotating and non-rotating planets. *J. Atmos. Sci.* **25**, 644–657.

WALIN, G. 1971 Contained non-homogeneous flow under gravity or how to stratify a fluid in the laboratory. *J. Fluid Mech.* **48**, 647–672.

WESSELING, P. 1969 Laminar convection cells at high Rayleigh number. *J. Fluid Mech.* **36**, 625–637.